

An Additive Overlapping Domain Decomposition Method for the Helmholtz Equation

Wei Leng ^{*} Lili Ju [†]

July 12, 2018

Abstract

In this paper, we propose and analyze an additive domain decomposition method (DDM) for solving the high-frequency Helmholtz equation with the Sommerfeld radiation condition. In the proposed method, the computational domain is partitioned into structured subdomains along all spatial directions, and each subdomain contains an overlapping region for source transferring. At each iteration all subdomain PML problems are solved completely in parallel, then all horizontal, vertical and corner directional residuals on each subdomain are passed to its corresponding neighbor subdomains as the source for the next iteration. This DDM method is highly scalable in nature and theoretically shown to produce the exact solution for the PML problem defined in \mathbb{R}^2 in the constant medium case. A slightly modified version of the method for bounded truncated domains is also developed for its use in practice and an error estimate is rigorously proved. Various numerical experiments in two and three dimensions are conducted on the supercomputer “Tianhe-2 Cluster” to verify the theoretical results and demonstrate excellent performance of the proposed method as an iterative solver or a preconditioner.

keywords

Additive domain decomposition method, Helmholtz equation, perfectly matching layer, convergence analysis, parallel computing

1 Introduction

In this paper, we consider the well-known Helmholtz equation in the space \mathbb{R}^n

$$\Delta u + k^2 u = f, \quad \text{in } \mathbb{R}^n \quad (1)$$

with the Sommerfeld radiation condition

$$r^{\frac{n-1}{2}} \left(\frac{\partial u}{\partial r} - iku \right) \rightarrow 0, \quad \text{as } r = |\mathbf{x}| \rightarrow \infty, \quad (2)$$

^{*}State Key Laboratory of Scientific and Engineering Computing, Chinese Academy of Sciences, Beijing 100190, China. Email: wleng@lsec.cc.ac.cn. W. Leng’s research is partially supported by Natural Science Foundation of China under grant number 11501553, and the National Center for Mathematics and Interdisciplinary Sciences of Chinese Academy of Sciences.

[†]Department of Mathematics, University of South Carolina, Columbia, SC 29208, USA. Email: ju@math.sc.edu. L. Ju’s research is partially supported by US National Science Foundation under grant number DMS-1521965.

where $u(\mathbf{x})$ is the unknown function, $f(\mathbf{x})$ is the source, $k(\mathbf{x})$ denotes the wave number, and $k(\mathbf{x}) = \omega/c(\mathbf{x})$, where ω is the angular frequency and $c(\mathbf{x})$ is the wave speed. Among many discretization and solution techniques for solving the Helmholtz equation (1), the domain decomposition method (DDM) [23, 24] is a very effective approach when the problem scale is very large and has been thoroughly studied for several decades. The basic idea is as follows: truncated with the absorbing boundary condition, the subdomain problem is (exactly or approximately) solved during each iteration, and the subdomain solutions is then passed to their respective neighbor subdomains via interface conditions to carry on the wave propagation process. The DDM is also especially popular to be used as a preconditioner to the iterative solver for the global discrete system.

The DDM was first used to solve the Helmholtz problem by Després in [25], and then various DDM algorithm has been developed to solve the Helmholtz problem [26, 27, 28, 29, 30, 31], these algorithm are categorized as the Schwarz methods with or without overlap. The boundary conditions at the subdomain interfaces affects the convergence of rate of the Schwarz method, thus Gander introduced the optimized Schwarz methods using an optimal non-local boundary condition [32, 33, 34, 35, 36, 37]. A non-overlapping Schwarz method was proposed by Boubendir et al. [38] using Padé approximations of the Dirichlet to Neumann (DtN) map, and the effective convergence is quasi-optimal.

The DDM with the transmission condition that involves sources yield fast methods to solve the high-frequency Helmholtz equation, the sweeping DDM preconditioner proposed by Engquist and Ying [9, 10] was the first of this type, and is shown to be very effective, and followed by the development of various sweeping type DDM, which differs mainly at the transmission condition at the interfaces of subdomains. The transmission condition of Engquist and Ying [9, 10] is that the residual in just one layer is taken as the source. The DDM introduced by Stolk [18] uses a transmission condition that the derivative of the solution is treated as a delta source. The double sweeping preconditioner developed by Vion and Geuzaine [19] uses a mixed boundary condition that involves DtN map as the transmission condition. The polarized trace method developed by Zepeda [22] impose a transmission condition that both single and double layer potentials are taken as delta sources. Instead of using the delta source approach, the source transfer DDM (STDDM) [4, 5] proposed by Chen and Xiang uses a smooth source coming from the residual as the transmission condition, and furthermore, an error estimate of the method has been rigorously proven. It is noted that the sweeping type DDMs often partition the domain in one direction, and the sweeping order would be along the direction forwards and backwards. Two orthogonal directions sweeping could be done in a recursive way, for instance, as proposed by Liu [16] using the sweeping preconditioner [9, 10], and by Wu [7] using the source transfer DDM [4, 5]. The sweeping type DDM is *multiplicative*, the subdomain problems are solved one after another in a particular order/direction, which could be interpreted as the process of LU or LDL^T factorization. The multiplicative DDMs usually have better convergence than the additive DDMs, however, the sequential sweeping order causes many difficulties to parallel computing in term of efficiency and scalability. In addition, the subdomain problems in the DDMs are often solved with direct solvers, such as the multi-frontal method [8, 14, 17], or the the multi-frontal method using hierarchically semiseparable structure [20, 21], but such one-direction partitions of the domain leave us large subdomains in practice and the robustness of the

direct solvers is still a challenge for such large size problems.

There are not many research on the of additive DDM with the transmission condition that involves sources for solving high-frequency Helmholtz equation. Liu and Ying proposed an additive sweeping preconditioner in [15], where the computational domain is partitioned in one direction into many thin layers, and the subproblems on all respective layers are solved in parallel with direct solvers. Wei introduced an additive overlapping DDM solver in [13], which uses a modified source transfer technique. The main advantages of the additive DDMs is that they are more suitable and scalable for parallel computing and much easier to implement on massively distributed machines than multiplicative ones. In this paper, we propose, analyze and test a new additive overlapping DDM for the Helmholtz equation (1) based on the source transfer technique [4]. We focus on illustrations of the DDM method on two-dimensional problems with constant medium, but it is very natural to use the method as an iterative solver or a preconditioner for the variable medium problems, and it is very straightforward to extend the proposed algorithm to three-dimensional problems. In our method, all the subdomain PML problems are solved completely in parallel at each iteration, and all *horizontal*, *vertical* and *corner* directional residuals on each subdomain are then passed to its corresponding neighbor subdomains as the source for the next iteration. Based on the source transfer analysis, the DDM method for the PML problem defined in \mathbb{R}^2 is theoretically shown to produce the exact solution in the constant medium case. Since the practical computations of the PML problems only can be done in bounded truncated domains, we then slightly modify the additive overlapping DDM to be useful for the truncated PML problem (which is an approximation to the full space problem). An error estimate of the method is further derived, and in particular, our proof revises and simplifies some analysis techniques used in [4] and successfully generalizes them to the additive type of DDM with the concurrent residual transfers in all directions.

The rest of the paper is organized as follows. In Section 2, we first present the additive overlapping DDM for the PML problem in the full space of \mathbb{R}^2 , and show that the DDM solution is exactly the solution to the problem in the constant medium case. In Section 3, the corresponding DDM in bounded truncated domains is then developed for practical use and its error estimate is also derived. In Section 4, various numerical experiments in two-dimensional and three-dimensional spaces are performed to verify the theoretical results and demonstrate effectiveness and scalability of the DDM method as an iterative solver or a preconditioner for the global discrete system. Some concluding remarks are finally drawn in Section 5.

2 The additive overlapping DDM in \mathbb{R}^2

In this section, the PML method and the source transfer technique are first briefly reviewed, then we will develop and analyze an additive overlapping DDM for solving the PML equation in the whole space \mathbb{R}^2 . The proposed DDM method will make use of the structured overlapping domain decomposition together with the source transfer in horizontal, vertical and corner directions. The constant medium problem (the constant wave number $k(\mathbf{x}) \equiv k$) is assumed for development and analysis of our DDM method.

2.1 Perfect match layer and source transfer

The solution of the Helmholtz equation (1) with the Sommerfeld radiation condition (2) in the constant medium case can be represented by

$$u(\mathbf{x}) = - \int_{\mathbb{R}^2} f(\mathbf{y}) G(\mathbf{x}, \mathbf{y}) d\mathbf{y}, \quad \forall \mathbf{x} \in \mathbb{R}^2, \quad (3)$$

where $G(\mathbf{x}, \mathbf{y}) = \frac{\mathbf{i}}{4} H_0^{(1)}(k|\mathbf{x} - \mathbf{y}|)$ is the fundamental solution of the Helmholtz equation defined by

$$\Delta G(\mathbf{x}, \mathbf{y}) + k^2 G(\mathbf{x}, \mathbf{y}) = -\delta_{\mathbf{y}}(\mathbf{x}), \quad \forall \mathbf{x} \in \mathbb{R}^2, \quad (4)$$

Note that $H_0^{(1)}(z)$, $z \in \mathbb{C}$ is often referred as the first Hankel function of order zero [1].

Consider a rectangular box $B = \{(x_1, x_2)^T : a_j \leq x_j \leq b_j, j = 1, 2\} \in \mathbb{R}^2$, and the center of the rectangle is denoted by (c_1, c_2) , where $c_j = \frac{a_j + b_j}{2}$, $j = 1, 2$. We will build and solve the PML equation in \mathbb{R}^2 for the rectangular box B , for instance, replace the solution outside B by the complex coordinate stretching as done in the so-called uniaxial PML method [6, 12, 2, 4]. Let $\alpha_1(x_1) = 1 + \mathbf{i}\sigma_1(x_1)$, $\alpha_2(x_2) = 1 + \mathbf{i}\sigma_2(x_2)$, with σ_1, σ_2 being piecewise smooth functions such that

$$\sigma_j(x) = \begin{cases} \tilde{\sigma}(x_j - b_j), & \text{if } b_j \leq x_j, \\ 0, & \text{if } a_j < x_j < b_j, \\ \tilde{\sigma}(a_j - x_j), & \text{if } x_j \leq a_j, \end{cases} \quad (5)$$

where $\tilde{\sigma}(t)$ is a smooth medium profile function satisfying that $\tilde{\sigma}(t) = \gamma_0$, for $t > d$, and both d and γ_0 are some positive constants. Then the complex coordinate stretching $\tilde{\mathbf{x}}(\mathbf{x})$ for $\mathbf{x} = (x_1, x_2)$ is defined as

$$\tilde{x}_j(x_j) = c_j + \int_{c_j}^{x_j} \alpha_j(t) dt = x_j + \mathbf{i} \int_{c_j}^{x_j} \sigma_j(t) dt, \quad j = 1, 2. \quad (6)$$

Denote $z^{1/2}$ the analytic branch of \sqrt{z} such that $\text{Re}(z^{1/2}) > 0$ for $z \in \mathbb{C}[0, +\infty]$, the distance in the complex plane is defined as

$$\rho(\tilde{\mathbf{x}}, \tilde{\mathbf{y}}) = [(\tilde{x}_1(x_1) - \tilde{y}_1(y_1))^2 + (\tilde{x}_2(x_2) - \tilde{y}_2(y_2))^2]^{1/2}. \quad (7)$$

Now we define

$$\tilde{u}(\mathbf{x}) = u(\tilde{\mathbf{x}}(\mathbf{x})) = - \int_{\mathbb{R}^2} f(\mathbf{y}) G(\tilde{\mathbf{x}}, \tilde{\mathbf{y}}) d\mathbf{y}, \quad \forall \mathbf{x} \in \mathbb{R}^2, \quad (8)$$

where $G(\tilde{\mathbf{x}}, \tilde{\mathbf{y}}) = \frac{\mathbf{i}}{4} H_0^{(1)}(k\rho(\tilde{\mathbf{x}}, \tilde{\mathbf{y}}))$. We also assume that f is compactly supported in B , then \tilde{u} is well-defined in $H_{loc}^1(\mathbb{R}^2)$, satisfies $\tilde{u}(\mathbf{x}) = u(\mathbf{x})$ in B , and decays exponentially as $|\mathbf{x}| \rightarrow \infty$. Consequently, it is the solution of the following PML equation with the source f :

$$J_B^{-1} \nabla \cdot (A_B \nabla \tilde{u}) + k^2 \tilde{u} = f, \quad \forall \mathbf{x} \in \mathbb{R}^2, \quad (9)$$

where $A_B(x) = \text{diag}\left(\frac{\alpha_2(x_2)}{\alpha_1(x_1)}, \frac{\alpha_1(x_1)}{\alpha_2(x_2)}\right)$ and $J_B(x) = \alpha_1(x_1)\alpha_2(x_2)$. We denote by $\mathcal{L}_B := J_B^{-1} \nabla \cdot (A_B \nabla \cdot) + k^2$ the linear operator associated with (9). The weak

formulation of the PML problem (9) can be given as follows: for $f \in H^1(\mathbb{R}^2)'$, find $u \in H^1(\mathbb{R}^2)$ such that

$$(A_B \nabla \tilde{u}, v) - k^2 (J_B \tilde{u}, v) = -\langle J_B f, v \rangle, \quad \forall v \in H^1(\mathbb{R}^2). \quad (10)$$

where (\cdot, \cdot) denotes the inner product in $L(\mathbb{R}^2)$ and $\langle \cdot \rangle$ the duality pairing between $H^1(\mathbb{R}^2)'$ and $H^1(\mathbb{R}^2)$. The well-posedness of the problem (10) has been established and could be found in [4, Lemma 3.3]. Let us denote by \mathcal{P}_B the above PML problem (10) associated with the rectangular box B .

The source transfer technique in \mathbb{R}^2 is briefly restated as follows. Suppose that \mathbb{R}^2 is divided into two parts Ω_1 and Ω_2 by the piecewise smooth curve γ , and at the same time γ also divides the rectangular box B into two parts. Let $\Omega_1^+ = \{\mathbf{x} : \rho(\mathbf{x}, \Omega_1) \leq \tilde{d}\}$, where \tilde{d} is a constant, and $\gamma^+ = \partial\Omega_1^+$, as show in Figure 1. There always exists a smooth function $\beta \in C^2(\mathbb{R}^2)$ such that

$$\beta|_{\Omega_1} \equiv 1, \quad \beta|_{\mathbb{R}^2 \setminus \Omega_1^+} \equiv 0, \quad 0 \leq \beta \leq 1,$$

and

$$|\nabla \beta(\mathbf{x})| < C, \quad \forall \mathbf{x} \in \Omega_1^+ \setminus \Omega_1,$$

where C denotes some generic positive constant.

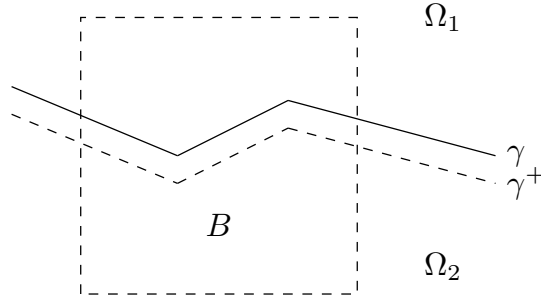


Figure 1: Divide \mathbb{R}^2 and the box B with γ .

It is quite straightforward to prove the following result. Denote by χ_{Ω_2} the characteristic function of Ω_2 .

Lemma 2.1. *Suppose the support of f is in $\Omega_1 \cap B$. Let u_0 be the solution to the PML problem \mathcal{P}_B with the source f (i.e., $\mathcal{L}_B u_0 = f$ in \mathbb{R}^2). Given $u_1 \in H^1(\mathbb{R}^2)$ such that $u_1 = u_0 \beta$ in \mathbb{R}^2 and let u_2 be solution to the PML problem \mathcal{P}_B with the source $-(\mathcal{L}_B u_1) \chi_{\Omega_2}$ (i.e., $\mathcal{L}_B u_2 = -(\mathcal{L}_B u_1) \chi_{\Omega_2}$ in \mathbb{R}^2). Then we have that $u_1 + u_2 = u_0$ in \mathbb{R}^2 and $u_2 = 0$ in Ω_1 .*

The two domains in Lemma 2.1 have an overlapping region $\Omega_1^+ \setminus \Omega_1$. For convenience, we shift the media profile function $\tilde{\sigma}(t)$ by \tilde{d} so that

$$\tilde{\sigma}(t) = \begin{cases} 0, & \text{if } t \leq \tilde{d} \\ \tilde{\sigma}(t - \tilde{d}), & \text{if } t > \tilde{d} \end{cases} \quad (11)$$

where $\tilde{\sigma}(t)$ is the shifted medium profile. From now on, we will denote $\tilde{\sigma}(t)$ as the above shifted medium profile for simplicity, and in this way, for the PML

problem \mathcal{P}_B , an extended region $\{\mathbf{x} : \rho(\mathbf{x}, B) \leq \tilde{d}\} \setminus B$ is always reserved as a possible overlapping region.

We will propose two types of source transfers in our method for the two-dimensional problem. Let κ_1 and κ_2 be two arbitrary constants such that $a_j \leq \kappa_j \leq b_j$, $j = 1, 2$. The first type is the transfer in x - or y -direction, as is shown in Figure 2 (left), where $\gamma = \{(x_1, x_2) : x_1 = \kappa_1\}$ or $\gamma = \{(x_1, x_2) : x_2 = \kappa_2\}$. We remark that such type of transfer is similar to the one used in STDDM [4]. The second type is the transfer in any of four corner directions, as is shown in Figure 2 (right), where $\gamma = \{(x_1, x_2) : x_1 = \kappa_1, x_2 \geq \kappa_2\} \cup \{(x_1, x_2) : x_1 \leq \kappa_1, x_2 = \kappa_2\}$. In both cases, we have $u_2 = 0$ in Ω_1 , therefore instead of solving the PML problem \mathcal{P}_B , we can turn to solve the PML problem $\mathcal{P}_{B \cap \Omega_2}$ whose solution is zero in Ω_1 .

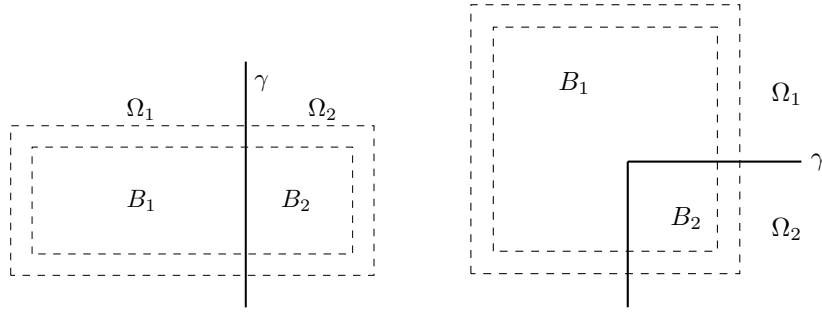


Figure 2: Source transfer in horizontal direction (left) and in the lower-right corner direction (right).

2.2 The DDM for the PML problem in \mathbb{R}^2

We now develop an additive overlapping DDM method to solve the PML equation (10) associated with a rectangular domain $\Omega = (-l_1, l_1) \times (-l_2, l_2)$ in \mathbb{R}^2 . Assume that Ω is uniformly partitioned into $N_1 \times N_2$ non-overlapping rectangular subdomains. Let $\Delta\xi = 2l_1/N_1$, $\xi_i = -l_1 + (i-1)\Delta\xi$, $i = 1, \dots, N_1+1$, and $\Delta\eta = 2l_2/N_2$, $\eta_j = -l_2 + (j-1)\Delta\eta$, $j = 1, \dots, N_2+1$. Then we have $N_1 \times N_2$ non-overlapping rectangular subdomains as

$$\Omega_{i,j} := [\xi_i, \xi_{i+1}] \times [\eta_j, \eta_{j+1}], \quad i = 1, 2, \dots, N_1, j = 1, 2, \dots, N_2.$$

It is clear that the PML equation associated with each rectangular subdomain $\Omega_{i,j}$ is needed to be solved in the DDM method. The source f , which is assumed to be compactly supported in Ω , is decomposed to

$$f_{i,j} = f \cdot \chi_{\Omega_{i,j}}, \quad i = 1, \dots, N_1, j = 1, \dots, N_2.$$

For convenience, we also define the box $\Omega_{i_0, i_1; j_0, j_1}$ ($1 \leq i_0 < i_1 \leq N_1+1$, $1 \leq j_0 < j_1 \leq N_2+1$), which consists of a set of rectangular subdomains as follows

$$\Omega_{i_0, i_1; j_0, j_1} := \bigcup_{\substack{i_0 \leq i \leq i_1 \\ j_0 \leq j \leq j_1}} \Omega_{i,j}.$$

Notice that the PML profile as (11) makes each subdomain has an overlapping region with its neighbor subdomains, thus we next define an overlapping domain decomposition of the two-dimensional space \mathbb{R}^2 as

$$\tilde{\Omega}_{i,j} := (\tilde{\xi}_i - \tilde{d}, \tilde{\xi}_{i+1} + \tilde{d}) \times (\tilde{\eta}_j - \tilde{d}, \tilde{\eta}_{j+1} + \tilde{d}), \quad i = 1, \dots, N_1, j = 1, \dots, N_2,$$

where

$$\tilde{\xi}_i = \begin{cases} -\infty, & i = 1, \\ \xi_i, & i = 2, \dots, N_1, \\ +\infty, & i = N_1 + 1, \end{cases} \quad \tilde{\eta}_j = \begin{cases} -\infty, & j = 1, \\ \eta_j, & j = 2, \dots, N_2, \\ +\infty, & j = N_2 + 1. \end{cases}$$

A few notations are introduced as follows. Let $\beta_0(t)$ be a monotone function in $C^2(\mathbb{R})$, such that $\beta_0(t) = 1$ for $t \leq 0$, $\beta_0(t) = 0$ for $t \geq 1$, and $|\beta'_0(t)| < C$ for $0 < t < 1$. Then define

$$\beta_{\leftarrow;i} = \begin{cases} 1, & i = 1, \\ \beta_0(\frac{\xi_i - x_1}{d}), & i = 2, \dots, N_1 + 1, \end{cases} \quad \beta_{\downarrow;j} = \begin{cases} 1, & j = 1, \\ \beta_0(\frac{\eta_j - x_2}{d}), & j = 2, \dots, N_2 + 1, \end{cases}$$

$$\beta_{\rightarrow;i} = \begin{cases} \beta_0(\frac{x_1 - \xi_i}{d}), & i = 1, \dots, N_1, \\ 1, & i = N_1 + 1, \end{cases} \quad \beta_{\uparrow;j} = \begin{cases} \beta_0(\frac{x_2 - \eta_j}{d}), & j = 1, \dots, N_2, \\ 1, & j = N_2 + 1, \end{cases}$$

and

$$\beta_{\swarrow;i,j} = \beta_{\leftarrow;i} \beta_{\downarrow;j}, \quad \beta_{\searrow;i,j} = \beta_{\rightarrow;i} \beta_{\downarrow;j},$$

$$\beta_{\nwarrow;i,j} = \beta_{\leftarrow;i} \beta_{\uparrow;j}, \quad \beta_{\nearrow;i,j} = \beta_{\rightarrow;i} \beta_{\uparrow;j}, \quad \beta_{0;i,j} = \beta_{\leftarrow;i} \beta_{\rightarrow;i+1} \beta_{\downarrow;j} \beta_{\uparrow;j+1}.$$

These functions will be used as β in Lemma 2.1 for different cases. Denote $\mathcal{L}_{i,j}$ as the linear operator associated with the PML problem $\mathcal{P}_{\Omega_{i,j}}$. Define the following characteristic functions for the half spaces and the quarter spaces:

$$\begin{aligned} \chi_{\leftarrow;i} &:= \chi(-\infty, \xi_i) \times (-\infty, +\infty), & \chi_{\rightarrow;i} &:= \chi(\xi_i, +\infty) \times (-\infty, +\infty), \\ \chi_{\downarrow;j} &:= \chi(-\infty, +\infty) \times (-\infty, \eta_j), & \chi_{\uparrow;j} &:= \chi(-\infty, +\infty) \times (\eta_j, +\infty), \\ \chi_{\swarrow;i,j} &:= \chi(-\infty, \xi_i) \times (-\infty, \eta_j), & \chi_{\searrow;i,j} &:= \chi(\xi_i, +\infty) \times (-\infty, \eta_j), \\ \chi_{\nwarrow;i,j} &:= \chi(-\infty, \xi_i) \times (\eta_j, +\infty), & \chi_{\nearrow;i,j} &:= \chi(\xi_i, +\infty) \times (\eta_j, +\infty). \end{aligned}$$

Using the β functions, characteristic functions and linear operators defined above, we are able to define the transfer operator as follows:

$$\begin{aligned} \Psi_{\leftarrow;i,j}(v) &:= -\mathcal{L}_{i-1,j}(\beta_{\leftarrow;i} v) \chi_{\leftarrow;i-1}, \\ \Psi_{\rightarrow;i,j}(v) &:= -\mathcal{L}_{i+1,j}(\beta_{\rightarrow;i+1} v) \chi_{\rightarrow;i+1}, \\ \Psi_{\downarrow;i,j}(v) &:= -\mathcal{L}_{i,j-1}(\beta_{\downarrow;j} v) \chi_{\downarrow;j-1}, \\ \Psi_{\uparrow;i,j}(v) &:= -\mathcal{L}_{i,j+1}(\beta_{\uparrow;j+1} v) \chi_{\uparrow;j+1}, \\ \Psi_{\swarrow;i,j}(v) &:= -\mathcal{L}_{i-1,j-1}(\beta_{\swarrow;i,j} v) \chi_{\swarrow;i-1,j-1}, \\ \Psi_{\searrow;i,j}(v) &:= -\mathcal{L}_{i+1,j-1}(\beta_{\searrow;i+1,j} v) \chi_{\searrow;i+1,j-1}, \\ \Psi_{\nwarrow;i,j}(v) &:= -\mathcal{L}_{i-1,j+1}(\beta_{\nwarrow;i,j+1} v) \chi_{\nwarrow;i-1,j+1}, \\ \Psi_{\nearrow;i,j}(v) &:= -\mathcal{L}_{i+1,j+1}(\beta_{\nearrow;i+1,j+1} v) \chi_{\nearrow;i+1,j+1}. \end{aligned}$$

Note that there are a total of $2^3 - 1 = 8$ directions for source transfer since each subdomain could have up to 8 neighbor subdomains in the two-dimensional space.

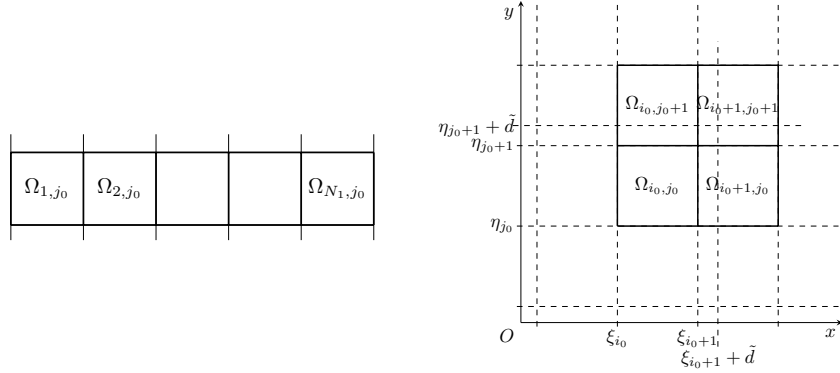


Figure 3: Source transfers in the horizontal direction (left) and in the upper-left corner direction (right) in the DDM.

First let us illustrate the source transfer in the *horizontal* or *vertical* direction of the domain decomposition. The procedure is essentially the same as the STDDM [4]. Assume $f_{1,j_0} \neq 0$, the PML problem $\mathcal{P}_{\Omega_{1,N_1;j_0,j_0}}$ with the source f_{1,j_0} is to be solved using the DDM, and its exact solution is denoted by u (see Figure 3 (left) for illustration). The subdomain PML problem on Ω_{i,j_0} can be solved in order from $i = 1$ to $i = N_1$ to construct the solution u : first, the problem $\mathcal{P}_{\Omega_{1,j_0}}$ with the source f_{1,j_0} is solved, the solution is denoted as u_1 , we have $u_1 = u$ in $\{(x_1, x_2) : x_1 \leq \xi_2 + \tilde{d}\}$; second, solve the PML problem $\mathcal{P}_{\Omega_{2,j_0}}$ with the source $\Psi_{\rightarrow;1,j_0}(u_1) = -\mathcal{L}_{2,j_0}(\beta_{\rightarrow;2}u_1)\chi_{\rightarrow;2}$, the solution is denoted u_2 , then using Lemma 2.1 on the box $\Omega_{1,2;j_0,j_0}$, we know that $u_1\beta_{\rightarrow;2} + u_2 = u$ in $\{(x_1, x_2) : x_1 \leq \xi_3 + \tilde{d}\}$; third, solve the PML problem $\mathcal{P}_{\Omega_{3,j_0}}$ with the source $\Psi_{\rightarrow;2,j_0}(u_2) = -\mathcal{L}_{3,j_0}(\beta_{\rightarrow;3}u_2)\chi_{\rightarrow;3}$, the solution is denoted u_3 , then using Lemma 2.1 on box $B_{1,3;j_0,j_0}$, we know that $u_1\beta_{\rightarrow;2} + u_2\beta_{\rightarrow;3} + u_3 = u$ in $\{(x_1, x_2) : x_1 \leq \xi_4 + \tilde{d}\}$; repeat the process until the last Box Ω_{N_1,j_0} , and the DDM solution is found as $\sum_{i=1,\dots,N_1} u_i\beta_{\rightarrow;i+1} = u$.

Remark 2.2. When the source transfer is in the horizontal or vertical direction, the source of the subdomain problem possesses a specific form. Let

$$\Phi_{m,i,j}(u; \beta) := J_{\Omega_{i,j}}^{-1} \frac{\partial}{\partial x_m} ((A_{\Omega_{i,j}})_{m,m} \frac{\partial \beta}{\partial x_m} u) + J_{\Omega_{i,j}}^{-1} \frac{\partial \beta}{\partial x_m} (A_{\Omega_{i,j}})_{m,m} \frac{\partial u}{\partial x_m}, \quad (12)$$

where $m = 1, 2$, then the above sources for the subdomain problem could be represented respectively as

$$\Psi_{\rightarrow;i,j_0}(u_i) = \Phi_{1;i+1,j_0}(u_i; \beta_{\rightarrow;i+1})\chi_{\rightarrow;i+1}, \quad i = 1, 2, \dots, N_1 - 1, \quad (13)$$

where the solution of other subdomain problem and its first order derivatives are involved but the wave number k is not. Similar forms exist for other horizontal or vertical directional source transfers.

Next we illustrate the source transfer in the corner directions of the domain decomposition. Suppose $f_{i_0,j_0} \neq 0$, the PML problem $\mathcal{P}_{\Omega_{i_0,i_0+1;j_0,j_0+1}}$ with the

source f_{i_0, j_0} is to be solved with the DDM, and its solution is denoted as u again (see Figure 3 (right) for illustration). First the solution to the PML problem $\mathcal{P}_{\Omega_{i_0, j_0}}$ with the source f_{i_0, j_0} is solved, and the solution is denoted as u_0 , obviously,

$$u_0 = u, \quad \text{in } \{(x_1, x_2) : x_1 \leq \xi_{i_0+1} + \tilde{d} \text{ and } x_2 \leq \eta_{j_0+1} + \tilde{d}\}. \quad (14)$$

Then the horizontal source transferring is applied, the problem $\mathcal{P}_{\Omega_{i_0+1, j_0}}$ with the source $\Psi_{\rightarrow; i_0, j_0}(u_0)$ is solved, and the solution is denoted as u_{\rightarrow} , we have

$$u_0 \beta_{\rightarrow; \xi_{i_0+1}} + u_{\rightarrow} = u, \quad \text{in } \{(x_1, x_2) : x_2 \leq \eta_{j_0} + \tilde{d}\}, \quad (15)$$

$$u_{\rightarrow} = 0, \quad \text{in } \{(x_1, x_2) : x_1 \leq \xi_{i_0}\}. \quad (16)$$

Similarly, the vertical source transferring is applied, the PML problem $\mathcal{P}_{\Omega_{i_0, j_0+1}}$ with the source $\Psi_{\uparrow; i_0, j_0}(u_0)$ is solved, and the solution is denoted as u_{\uparrow} , we have

$$u_0 \beta_{\uparrow; \eta_{j_0+1}} + u_{\uparrow} = u, \quad \text{in } \{(x_1, x_2) : x_1 \leq \xi_{i_0} + \tilde{d}\}, \quad (17)$$

$$u_{\uparrow} = 0, \quad \text{in } \{(x_1, x_2) : x_2 \leq \eta_{j_0}\}. \quad (18)$$

By (14)-(18), we obtain that

$$u_0 \beta_{\nearrow; \xi_{i_0+1, j_0+1}} + u_{\rightarrow} \beta_{\uparrow; \eta_{j_0+1}} + u_{\uparrow} \beta_{\rightarrow; \xi_{i_0+1}} = u(\beta_{\rightarrow; \xi_{i_0+1}} + \beta_{\uparrow; \eta_{j_0+1}} - \beta_{\nearrow; \xi_{i_0+1, j_0+1}}), \quad \text{in } \mathbb{R}^2. \quad (19)$$

At last the PML problem $\mathcal{P}_{\Omega_{i_0+1, j_0+1}}$ with the source

$$\begin{aligned} & -\mathcal{L}_{B_{i_0, i_0+1; j_0, j_0+1}}(u(\beta_{\rightarrow; \xi_{i_0+1}} + \beta_{\uparrow; \eta_{j_0+1}} - \beta_{\nearrow; \xi_{i_0+1, j_0+1}})) \chi_{\nearrow; i_0+1, j_0+1}, \\ & = -\mathcal{L}_{i_0+1, j_0+1}(u_0 \beta_{\nearrow; \xi_{i_0+1, j_0+1}} + u_{\rightarrow} \beta_{\uparrow; \eta_{j_0+1}} + u_{\uparrow} \beta_{\rightarrow; \xi_{i_0+1}}) \chi_{\nearrow; i_0+1, j_0+1} \\ & = \left(\Psi_{\nearrow; i_0, j_0}(u_0) + \Psi_{\uparrow; i_0+1, j_0}(u_{\rightarrow}) + \Psi_{\rightarrow; i_0, j_0+1}(u_{\uparrow}) \right) \chi_{\nearrow; i_0+1, j_0+1}, \end{aligned} \quad (20)$$

is solved and the solution is denoted as u_{\nearrow} . Observe that

$$\begin{aligned} & \beta_{\rightarrow; \xi_{i_0+1}} + \beta_{\uparrow; \eta_{j_0+1}} - \beta_{\nearrow; \xi_{i_0+1, j_0+1}} = 1 - (1 - \beta_{\rightarrow; \xi_{i_0+1}})(1 - \beta_{\uparrow; \eta_{j_0+1}}) \\ & = \begin{cases} 1 & \text{in } \{(x_1, x_2) : x_1 \leq \xi_{i_0+1} \text{ or } x_2 \leq \eta_{j_0+1}\}, \\ 0 & \text{in } \{(x_1, x_2) : x_1 \geq \xi_{i_0+1} + \tilde{d} \text{ and } x_2 \geq \eta_{j_0+1} + \tilde{d}\}. \end{cases} \end{aligned}$$

Using Lemma 2.1 on the box $\Omega_{i_0, i_0+1; j_0, j_0+1}$, the DDM solution is found to be

$$u = u_0 \beta_{\nearrow; \xi_{i_0+1, j_0+1}} + u_{\rightarrow} \beta_{\uparrow; \eta_{j_0+1}} + u_{\uparrow} \beta_{\rightarrow; \xi_{i_0+1}} + u_{\nearrow}.$$

Remark 2.3. When the source transfer is in the corner directions, the source for the subdomain problem also has a specific form, e.g., the source (20) could be represented as

$$\begin{aligned} & \left(\Phi_{1; i_0+1, j_0+1}(u_{\uparrow}; \beta_{\rightarrow; i_0+1}) + \Phi_{2; i_0+1, j_0+1}(u_{\rightarrow}; \beta_{\uparrow; j_0+1}) \right. \\ & \left. + \Phi_{1; i_0+1, j_0+1}(u_0; \beta_{\nearrow; i_0+1}) + \Phi_{2; i_0+1, j_0+1}(u_0; \beta_{\nearrow; j_0+1}) \right) \chi_{\nearrow; i_0+1, j_0+1}, \end{aligned} \quad (21)$$

where the solutions of other subdomain problems and their first order derivatives are again involved but the wave number k is not. Similar forms exist for other corner directional source transfers. Also such source transfer in the corner directions could be generalized to the case of more subdomains.

With the source transfer in horizontal, vertical and corner directions as shown above, the solution to the PML problem \mathcal{P}_Ω with the source f_{i_0, j_0} could be constructed by induction, the details are omitted here. For the general source $f = \sum_{\substack{i=1, \dots, N_1 \\ j=1, \dots, N_2}} f_{i,j}$, the solution process for each source $f_{i,j}$ can be handled concurrently, thus we propose an additive overlapping DDM for the PML problem as below.

Algorithm 2.1 (Additive overlapping DDM for the PML problem \mathcal{P}_Ω with the source f).

- Set $\{u_{i,j}^0\} = 0$ in \mathbb{R}^2 for $i = 1, 2, \dots, N_1, j = 1, 2, \dots, N_2$.
- Step 1: solve the PML problem $\mathcal{P}_{\Omega_{i,j}}$ with the source $f_{i,j}$

$$\mathcal{L}_{i,j} u_{i,j}^1 = f_{i,j}, \quad \text{in } \mathbb{R}^2, \quad (22)$$

for $i = 1, 2, \dots, N_1, j = 1, 2, \dots, N_2$.

- For Step $s = 2, 3, \dots, N_1 + N_2$: solve

$$\begin{aligned} \mathcal{L}_{i,j} u_{i,j}^s = & \Psi_{\leftarrow; i+1, j}(u_{i+1, j}^{s-1}) + \Psi_{\rightarrow; i-1, j}(u_{i-1, j}^{s-1}) \\ & + \Psi_{\downarrow; i, j+1}(u_{i, j+1}^{s-1}) + \Psi_{\uparrow; i, j-1}(u_{i, j-1}^{s-1}) \\ & + \Psi_{\swarrow; i+1, j+1}(u_{i+1, j+1}^{s-2}) + \Psi_{\searrow; i-1, j+1}(u_{i-1, j+1}^{s-2}) \\ & + \Psi_{\nwarrow; i+1, j-1}(u_{i+1, j-1}^{s-2}) + \Psi_{\nearrow; i-1, j-1}(u_{i-1, j-1}^{s-2}), \quad \text{in } \mathbb{R}^2, \end{aligned} \quad (23)$$

for $i = 1, 2, \dots, N_1, j = 1, 2, \dots, N_2$.

- The DDM solution for \mathcal{P}_Ω with the source f is then given by

$$u_{DDM} = \sum_{\substack{i=1, \dots, N_1 \\ j=1, \dots, N_2}} \beta_{0; i, j} u_{i, j} \quad (24)$$

$$\text{with } u_{i, j} = \sum_{s=1, \dots, N_1+N_2} u_{i, j}^s.$$

Theorem 2.4. $u_{DDM}(f) = u(f)$ where $u(f)$ is the solution of the PML problem \mathcal{P}_Ω with the source f and $u_{DDM}(f)$ is the corresponding DDM solution constructed by Algorithm 2.1.

Proof: Obviously, $u_{DDM}(f) = \sum_{\substack{i=1, \dots, N_1 \\ j=1, \dots, N_2}} u_{DDM}(f_{i,j})$. Hence to show that $u_{DDM}(f)$ is the solution to the problem \mathcal{P}_Ω with the source f , we only need to show that for any $i_0 \in \{1, \dots, N_1\}, j_0 \in \{1, \dots, N_2\}$, $u_{DDM}(f_{i_0, j_0})$ is the solution to \mathcal{P}_Ω with the source $f(i_0, j_0)$, denoted as $u(f_{i_0, j_0})$.

At Step 1, only the solution of subdomain Ω_{i_0, j_0} , u_{i_0, j_0}^1 , need to be updated with (22) ($u_{i,j}^1 = 0$ for $i \neq i_0$ or $j \neq j_0$ due to zero source).

At Step 2, based on (23), on the subdomains $\Omega_{i,j}$ with $|i - i_0| + |j - j_0| + 1 = 2$, $u_{i,j}^2$'s are computed with horizontal or vertical source transfers. For instance, on the subdomain Ω_{i_0+1, j_0} , omitting the zero terms in the RHS of (23),

$$\mathcal{L}_{i_0+1, j_0} u_{i_0+1, j_0}^2 = \Psi_{\rightarrow; i_0, j_0}(u_{i_0, j_0}^1). \quad (25)$$

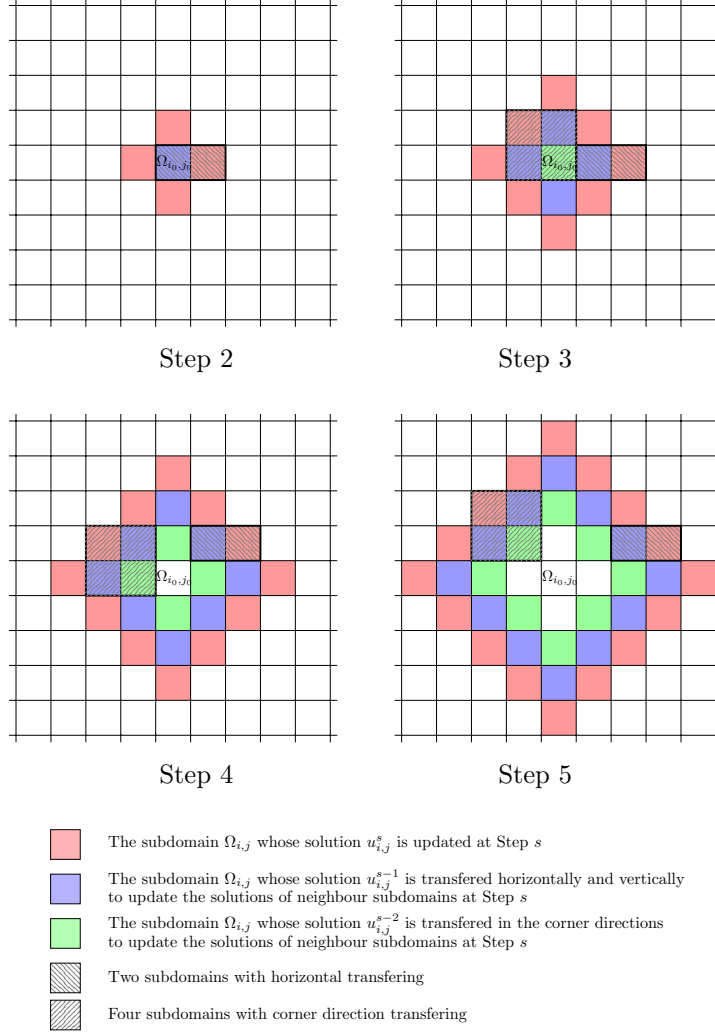


Figure 4: The updating process of the subdomain solutions at Steps 2, 3, 4, 5 in the additive overlapping DDM for the PML problem \mathcal{P}_Ω with the source $f(i_0, j_0)$.

Using the analysis of horizontal and vertical directional source transfers, we have that

$$\sum_{\substack{r=1,2 \\ |i-i_0|+|j-j_0|+1 \leq 2}} u_{i,j}^r \beta_{0;i,j} = u(f_{i_0,j_0}), \quad \text{in } \bigcup_{|i-i_0|+|j-j_0|+1 \leq 2} \Omega_{i,j} \quad (26)$$

as is shown in Figure 4 (top-left). Note that there is no reflections opposite to the propagating direction – let us take the subdomain Ω_{i_0+1,j_0} for example, with the horizontal updating (25), u_{i_0+1,j_0}^2 is a right going (\rightarrow) wave solution, thus by Lemma 2.1, $\Psi_{\square;i_0+1,j_0}(u_{i_0+1,j_0}^2) = 0$, for $\square = \leftarrow, \nwarrow, \swarrow$.

At Step 3, based on (23), on the subdomains $\Omega_{i,j}$ with $|i-i_0|+|j-j_0|+1 \leq 3$, $u_{i,j}^2$'s are computed. However, since there is no reflections opposite to the prop-

agating direction, only those on the subdomains $\Omega_{i,j}$ with $|i-i_0|+|j-j_0|+1=3$ really need to be updated. The solutions on the subdomains $\Omega_{i_0\pm 2,j_0}$ and $\Omega_{i_0,j_0\pm 2}$ are updated with horizontal or vertical source transfers, respectively; the solutions on the subdomains $\Omega_{i_0\pm 1,j_0\pm 1}$ are updated with horizontal, vertical and corner directional source transfers. For instance, on the subdomain Ω_{i_0-1,j_0+1} , omitting the zero terms in the RHS of (23),

$$\mathcal{L}_{i_0-1,j_0+1}u_{i_0-1,j_0+1}^3 = \Psi_{\leftarrow;i_0,j_0+1}(u_{i_0,j_0+1}^2) + \Psi_{\uparrow;i_0-1,j_0}(u_{i_0-1,j_0}^2) + \Psi_{\nwarrow;i_0,j_0}(u_{i_0,j_0}^1). \quad (27)$$

Using the analysis of horizontal, vertical and corner directional source transfers, we have that

$$\sum_{\substack{r=1,\dots,3 \\ |i-i_0|+|j-j_0|+1\leq 3}} u_{i,j}^r \beta_{0;i,j} = u(f_{i_0,j_0}), \quad \text{in } \bigcup_{|i-i_0|+|j-j_0|+1\leq 3} \Omega_{i,j} \quad (28)$$

as is shown in Figure 4 (top-right). Again, there is no reflections opposite to the propagating direction for the horizontal, vertical and corner directional transfers: the case of horizontal and vertical solution updating are similar to Step 2; for the case of corner direction solution updating, let us take the subdomain Ω_{i_0-1,j_0+1} for example, with the corner directional updating (27), u_{i_0-1,j_0+1}^2 is a up-left going (\nwarrow) wave solution, thus by Lemma 2.1, $\Psi_{\square;i_0-1,j_0+1}(u_{i_0-1,j_0+1}^2) = 0$ for $\square = \rightarrow, \downarrow, \nearrow, \swarrow, \searrow$.

Repeat the procedure (see the bottom panel of Figure 4), we always have

$$\sum_{\substack{r=1,\dots,s \\ |i-i_0|+|j-j_0|+1\leq s}} u_{i,j}^r \beta_{0;i,j} = u(f_{i_0,j_0}), \quad \text{in } \bigcup_{|i-i_0|+|j-j_0|+1\leq s} \Omega_{i,j}. \quad (29)$$

Hence we finally have $u_{\text{DDM}}(f_{i_0,j_0}) = u(f_{i_0,j_0})$ after Step $N_1 + N_2$. \square

3 The additive overlapping DDM in bounded truncated domains

In this section, the additive overlapping DDM in a bounded truncated domain is proposed based on the DDM in the full space of \mathbb{R}^2 in the preceding section. Again the constant medium problem is assumed, and an error estimate of the method is established. First some notations are introduced as in [4]. For any bounded domain $U \in \mathbb{R}^2$ with Lipschitz boundary Γ , we define the following norms:

$$\begin{aligned} \|u\|_{H^1(U)} &= \left(\|\nabla u\|^2 + \|ku\|_{L^2(U)}^2 \right)^{1/2}, \\ \|u\|_{H^1(U)} &= \left(\|\nabla u\|^2 + d_U^{-2} \|u\|_{L^2(U)}^2 \right)^{1/2}, \\ |v|_{\frac{1}{2},\Gamma}^2 &= \int_{\Gamma} \int_{\Gamma} \frac{|v(x) - v(x')|^2}{|x - x'|^2} ds(x) ds(x'), \\ \|v\|_{H^{1/2}(\Gamma)} &= \left(d_U^{-1} \|\nabla v\|_{L^2(\Gamma)}^2 + |v|_{\frac{1}{2},\Gamma}^2 \right)^{1/2}, \end{aligned}$$

where $d_U = \text{diam}(U)$. Obviously,

$$\|v\|_{H^{\frac{1}{2}}(\Gamma)} \leq (|\Gamma|d_U^{-1})^{\frac{1}{2}}\|v\|_{L^\infty(\Gamma)} + |\Gamma| \|\nabla v\|_{L^\infty(\Gamma)}, \quad \forall v \in W^{1,\infty}(\Gamma). \quad (30)$$

Using the scaling argument and trace theorem we have for any $v \in H^{\frac{1}{2}}(\Gamma)$,

$$C_1 \frac{|U|^{\frac{1}{2}}}{|\Gamma|} \|v\|_{H^{\frac{1}{2}}(\Gamma)} \leq \inf_{\substack{\phi|_{\Gamma}=v \\ \phi \in H^1(U)}} \|\phi\|_{H^1(U)} \leq C_2 \frac{|U|^{\frac{1}{2}}}{|\Gamma|} \|v\|_{H^{\frac{1}{2}}(\Gamma)}, \quad (31)$$

where $C_1, C_2 > 0$ are constants independent of d_U .

3.1 The DDM for the truncated PML problem

Given any rectangular domain $\Omega = [-l_1, l_1] \times [-l_2, l_2] \in \mathbb{R}^2$, let us define an extended box $\Omega^{\text{PML}} = [-l_1 - d, l_1 + d] \times [-l_2 - d, l_2 + d]$ with $d > \tilde{d}$. Then the weak formulation of the truncated PML problem associated with Ω (denoted by $\widehat{\mathcal{P}}_\Omega$) is defined by: for $f \in H^1(\Omega)'$, find $\hat{u} \in H_0^1(\Omega^{\text{PML}})$ such that

$$(A_\Omega \nabla \hat{u}, v) - k^2 (J_\Omega \hat{u}, v) = -\langle J_\Omega f, v \rangle, \quad \forall v \in H^1(\Omega^{\text{PML}}). \quad (32)$$

Define $L = \max(l_1 + d, l_2 + d)$. we consider solve the above truncated PML problem $\widehat{\mathcal{P}}_\Omega$ with the source f using the additive overlapping DDM.

It is proved in [4, Lemma 3.4], that for sufficiently large $\sigma_0 d \geq 1$, where $\sigma_0 = \max_{t \in \mathbb{R}} \tilde{\sigma}(t)$, the sesquilinear form associated with the above truncated PML problem (32) satisfies the inf-sup condition: there exists a positive constant $\mu^{-1} \leq Ck^{\frac{3}{2}}$ such that

$$\sup_{\psi \in H_0^1(\Omega^{\text{PML}})} \frac{|(A_\Omega \nabla \phi, \nabla \psi) - k^2 (J_\Omega \phi, \psi)|}{\|\psi\|_{H^1(\Omega^{\text{PML}})}} \geq \mu \|\phi\|_{H^1(\Omega^{\text{PML}})}, \quad \forall \phi \in H_0^1(\Omega^{\text{PML}}). \quad (33)$$

The solution of the truncated PML problem $\widehat{\mathcal{P}}_\Omega$, denoted as \hat{u} , is an approximation of the solution u of the PML problem \mathcal{P}_Ω , and the following error estimate has been proven,

$$\|u - \hat{u}\|_{H^1(\Omega^{\text{PML}})} \leq Ck^2(1 + kL)^2 e^{-\frac{1}{2}k\gamma_0\bar{\sigma}}, \quad (34)$$

where $\gamma_0 = \frac{d}{\sqrt{d^2 + 4((b_1 - a_1) + (b_2 - a_2) + d)^2}}$, and $\bar{\sigma} = \int_0^d \tilde{\sigma}(t)dt$. It is clear that \hat{u} is zero on $\partial\Omega^{\text{PML}}$, while u is not. However, as is shown in the proof of [4, Lemma 3.4], we have the following estimate for that

$$|u(\mathbf{x})| \leq Ck^{1/2} e^{-\frac{1}{2}k\gamma_0\bar{\sigma}} \|f\|_{H^1(\Omega)'}, \quad \forall \mathbf{x} \in \partial\Omega^{\text{PML}}, \quad (35)$$

$$|\nabla u(\mathbf{x})| \leq Ck^{3/2} e^{-\frac{1}{2}k\gamma_0\bar{\sigma}} \|f\|_{H^1(\Omega)'}, \quad \forall \mathbf{x} \in \partial\Omega^{\text{PML}}. \quad (36)$$

The truncated PML problem that we solved in this paper is for each subdomain $\Omega_{i,j}$ ($\Omega_{i,j} \subset \Omega$), therefore we use the same $\gamma_0 = \frac{d}{\sqrt{d^2 + 4(l_1 + l_2 + d)^2}}$ for all truncated subdomain PML problems in the rest of the paper.

Denote $\widehat{\mathcal{L}}_{i,j}$ as the operator associated with the truncated subdomain PML problem $\widehat{\mathcal{P}}_{\Omega_{i,j}}$. Substitute PML problem operator $\mathcal{L}_{i,j}$ with $\widehat{\mathcal{L}}_{i,j}$, solution $u_{\square;i,j}$ with $\hat{u}_{\square;i,j}$ in Algorithm 2.1, we have the correspondingly revised DDM for the truncated PML problem in \mathbb{R}^2 ,

Algorithm 3.1 (Additive overlapping DDM for the truncated PML problem $\widehat{\mathcal{P}}_\Omega$ with the source f).

- Set $\{\hat{u}_{i,j}^0\} = 0$ in $\Omega_{i,j}^{PML}$ for $i = 1, 2, \dots, N_1$, $j = 1, 2, \dots, N_2$.
- Step 1: solve the truncated PML problem $\widehat{\mathcal{P}}_{\Omega_{i,j}}$ with the source $f_{i,j}$

$$\widehat{\mathcal{L}}_{i,j} \hat{u}_{i,j}^1 = f_{i,j}, \quad \text{in } \Omega_{i,j}^{PML}, \quad (37)$$

for $i = 1, 2, \dots, N_1$, $j = 1, 2, \dots, N_2$.

- For Step $s = 2, 3, \dots, N_1 + N_2$: solve

$$\begin{aligned} \widehat{\mathcal{L}}_{i,j} \hat{u}_{i,j}^s = & \Psi_{\leftarrow; i+1, j}(\hat{u}_{i+1, j}^{s-1}) + \Psi_{\rightarrow; i-1, j}(\hat{u}_{i-1, j}^{s-1}) \\ & + \Psi_{\downarrow; i, j+1}(\hat{u}_{i, j+1}^{s-1}) + \Psi_{\uparrow; i, j-1}(\hat{u}_{i, j-1}^{s-1}) \\ & + \Psi_{\swarrow; i+1, j+1}(\hat{u}_{i+1, j+1}^{s-2}) + \Psi_{\searrow; i-1, j-1}(\hat{u}_{i-1, j-1}^{s-2}) \\ & + \Psi_{\nwarrow; i+1, j-1}(\hat{u}_{i+1, j-1}^{s-2}) + \Psi_{\nearrow; i-1, j+1}(\hat{u}_{i-1, j+1}^{s-2}), \quad \text{in } \Omega_{i,j}^{PML}, \end{aligned} \quad (38)$$

for $i = 1, 2, \dots, N_1$, $j = 1, 2, \dots, N_2$.

- The DDM solution for $\widehat{\mathcal{P}}_\Omega$ with the source f is then given by

$$\hat{u}_{DDM}(f) = \sum_{\substack{i=1, \dots, N_1 \\ j=1, \dots, N_2}} \beta_{0; i, j} \hat{u}_{i, j} \quad (39)$$

$$\text{with } \hat{u}_{i, j} = \sum_{s=1, \dots, N_1+N_2} \hat{u}_{i, j}^s.$$

Remark 3.1. The additive overlapping DDM algorithms (Algorithms 2.1 and 3.1) can be straightforwardly generalized to solve the three-dimensional PML and truncated PML problems, where there are now a total of $3^3 - 1 = 26$ directions for source transfer and $N_1 + N_2 + N_3$ iteration steps (N_3 denotes the number of partitions in the z -direction).

3.2 Error estimate

Let us first only consider the case of only the source $f_{i_0, j_0} \neq 0$. Then it holds that the subdomain solution $u_{i, j}^s$ is non-zero only at Step $s = |i - i_0| + |j - j_0| + 1$, while the subdomain solution $\hat{u}_{i, j}^s$ is non-zero at Steps $s \geq |i - i_0| + |j - j_0| + 1$.

Lemma 3.2. Assume that only the source $f_{i_0, j_0} \neq 0$ and $\sigma_0 d$ be sufficiently large. For $i = 1, \dots, N_1$, $j = 1, \dots, N_2$, it holds

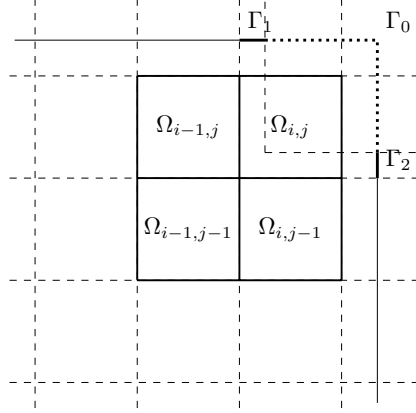
$$\|u_{i, j}^s\|_{H^{1/2}(\partial\Omega_{i, j}^{PML})} \leq C k^{\frac{1}{2}} (1 + kL) e^{-\frac{1}{2} k \gamma_0 \bar{\sigma}} \|f_{i_0, j_0}\|_{H^1(B_l)'}, \quad (40)$$

for $s = |i - i_0| + |j - j_0| + 1$.

Proof: First we prove that

$$|u_{i, j}^s(\mathbf{x})| \leq C k^{\frac{1}{2}} e^{-\frac{1}{2} k \gamma_0 \bar{\sigma}} \|f_{i_0, j_0}\|_{H^1(B_l)'}, \quad \forall \mathbf{x} \in \partial\Omega_{i, j}^{PML}, \quad (41)$$

$$|\nabla u_{i, j}^s(\mathbf{x})| \leq C k^{\frac{3}{2}} e^{-\frac{1}{2} k \gamma_0 \bar{\sigma}} \|f_{i_0, j_0}\|_{H^1(B_l)'}, \quad \forall \mathbf{x} \in \partial\Omega_{i, j}^{PML}. \quad (42)$$

Figure 5: $\Gamma_0, \Gamma_1, \Gamma_2$.

Consider the case $i \geq i_0 + 1, j \geq j_0 + 1$ for example. Denote by $u_{i_0,i;j_0,j}$ the solution to the PML problem $\mathcal{P}_{\Omega_{i_0,i;j_0,j}}$ with f_{i_0,j_0} as the source, then we have by (35)-(36)

$$|u_{i_0,i;j_0,j}| \leq Ck^{\frac{1}{2}}e^{-\frac{1}{2}k\gamma_0\bar{\sigma}}\|f_{i_0,j_0}\|_{H^1(B_l)'}, \quad \forall \mathbf{x} \in \partial B_{i_0,i;j_0,j}. \quad (43)$$

$$|\nabla u_{i_0,i;j_0,j}| \leq Ck^{\frac{3}{2}}e^{-\frac{1}{2}k\gamma_0\bar{\sigma}}\|f_{i_0,j_0}\|_{H^1(B_l)'}, \quad \forall \mathbf{x} \in \partial B_{i_0,i;j_0,j}. \quad (44)$$

Define $\Gamma_0 = \partial\Omega_{i,j}^{\text{PML}} \cap \{x_1 \geq \xi_i + d, x_2 \geq \eta_j + d\}$, $\Gamma_1 = \{\xi_i \leq x_1 \leq \xi_i + d, x_2 = \eta_{j+1} + d\}$, $\Gamma_2 = \{x_1 = \xi_{i+1} + d, \eta_j \leq x_2 \leq \eta_{j+1} + d\}$, as shown in Figure 5. By Lemma 2.1, $u_{i,j}^s$ is zero on $\partial\Omega_{i_0,i;j_0,j}$ except for $\Gamma_0 \cup \Gamma_1 \cup \Gamma_2$, moreover, by (19),

$$\begin{aligned} u_{i,j}^s &= u_{i_0,i;j_0,j}, & \text{on } \Gamma_0, \\ u_{i,j}^s &= u_{i_0,i;j_0,j}(1 - \beta_{\rightarrow;i_0}), & \text{on } \Gamma_1, \\ u_{i,j}^s &= u_{i_0,i;j_0,j}(1 - \beta_{\uparrow;j_0}), & \text{on } \Gamma_2, \end{aligned}$$

which imply (41)-(42) together with (43)-(44).

By (30) we then obtain

$$\|u_{i,j}^s\|_{H^{1/2}(\partial\Omega_{i,j}^{\text{PML}})} \leq C \max_{x \in \partial\Omega_{i,j}^{\text{PML}}} (|u_{i,j}^s| + L|\nabla u_{i,j}^s|), \quad (45)$$

which further gives us (40) by using (41) and (42). \square

Lemma 3.3. Assume that only the source $f_{i_0,j_0} \neq 0$ and $\sigma_0 d$ be sufficiently large. For $i = 1, \dots, N_1, j = 1, \dots, N_2$, it holds

$$\|u_{i,j}^s - \hat{u}_{i,j}^s\|_{H^1(\Omega_{i,j}^{\text{PML}})} \leq Ck^{\frac{3}{2}s+\frac{1}{2}}(1+kL)^2e^{-\frac{1}{2}k\gamma_0\bar{\sigma}}\|f_{i_0,j_0}\|_{H^1(\Omega)'}. \quad (46)$$

Proof: Let the source of the PML problem $\mathcal{P}_{\Omega_{i,j}}$ at Step s in (22)-(23) of the DDM Algorithm 2.1 be denoted as $f_{i,j}^s$, and the source for the truncated PML problem $\hat{\mathcal{P}}_{\Omega_{i,j}}$ at Step s in (37)-(38) of the DDM algorithm 3.1 be denoted as $\hat{f}_{i,j}^s$.

First we will prove the following error estimate for the source in the DDM Algorithm by induction

$$\|f_{i,j}^s - \hat{f}_{i,j}^s\|_{H^1(\Omega_{i,j}^{\text{PML}})} \leq Ck^{\frac{3}{2}s-1}(1+kL)^2 e^{-\frac{1}{2}k\gamma_0\bar{\sigma}} \|f_{i_0,j_0}\|_{H^1(\Omega)'} \quad (47)$$

Obviously (47) holds for $s = 1$ since $f_{i,j}^1 = \hat{f}_{i,j}^1$, suppose it holds for $s = 2, \dots, t-1$, we will prove it also holds for $s = t$. By the analysis of source transfers in horizontal, vertical and corner directions, we know that the sources of the subdomain problems have other forms that involve the solutions of other subdomain problems and their first-order derivatives but not k . This indicates

$$\begin{aligned} \|f_{i,j}^t - \hat{f}_{i,j}^t\|_{H^{-1}(\Omega_{i,j}^{\text{PML}})} &\leq \sum_{(i',j')=(i\pm 1,j),(i,j\pm 1)} \|u_{i',j'}^{t-1} - \hat{u}_{i',j'}^{t-1}\|_{H^1(\Omega_{i',j'}^{\text{PML}})} \\ &+ \sum_{(i',j')=(i\pm 1,j+1),(i\pm 1,j-1)} \|u_{i',j'}^{t-2} - \hat{u}_{i',j'}^{t-2}\|_{H^1(\Omega_{i',j'}^{\text{PML}})}. \end{aligned} \quad (48)$$

Take $\|u_{i+1,j}^{t-1} - \hat{u}_{i+1,j}^{t-1}\|_{H^1(\Omega_{i+1,j}^{\text{PML}})}$ for example, by (31), there exists a lifting function $\phi \in H^1(\Omega_{i+1,j}^{\text{PML}})$ that $\phi = u_{i+1,j}^{t-1}$ on $\partial\Omega_{i+1,j}^{\text{PML}}$, and $\|\phi\|_{H^1(\Omega_{i+1,j}^{\text{PML}})} \leq C\|u_{i+1,j}^{t-1}\|_{H^{\frac{1}{2}}(\partial\Omega_{i+1,j}^{\text{PML}})}$. Note that $u_{i+1,j}^{t-1} - \hat{u}_{i+1,j}^{t-1} - \phi \in H_0^1(\Omega_{i+1,j}^{\text{PML}})$, then by (33), we have

$$\begin{aligned} \|u_{i+1,j}^{t-1} - \hat{u}_{i+1,j}^{t-1} - \phi\|_{H^1(\Omega_{i+1,j}^{\text{PML}})} &\leq \mu^{-1} \left(\sup_{\psi \in H_0^1(\Omega_{i+1,j}^{\text{PML}})} \frac{|(A_{\Omega_{i+1,j}} \nabla \phi, \nabla \psi) - k^2 (J_{\Omega_{i+1,j}} \phi, \psi)|}{\|\psi\|_{H^1(\Omega_{i+1,j}^{\text{PML}})}} \right. \\ &\quad \left. + \|f_{i+1,j}^{t-1} - \hat{f}_{i+1,j}^{t-1}\|_{H^{-1}(\Omega_{i+1,j}^{\text{PML}})} \right) \\ &\leq C\mu^{-1} \left(\|\phi\|_{H^1(\Omega_{i+1,j}^{\text{PML}})} + \|f_{i+1,j}^{t-1} - \hat{f}_{i+1,j}^{t-1}\|_{H^{-1}(\Omega_{i+1,j}^{\text{PML}})} \right), \end{aligned}$$

therefore we have

$$\begin{aligned} \|u_{i+1,j}^{t-1} - \hat{u}_{i+1,j}^{t-1}\|_{H^1(\Omega_{i+1,j}^{\text{PML}})} &\leq Ck^{\frac{3}{2}} \|f_{i+1,j}^{t-1} - \hat{f}_{i+1,j}^{t-1}\|_{H^{-1}(\Omega_{i+1,j}^{\text{PML}})} + Ck^{\frac{3}{2}}(1+kL) \|\phi\|_{H^1(\Omega_{i+1,j}^{\text{PML}})} \\ &\leq Ck^{\frac{3}{2}} \|f_{i+1,j}^{t-1} - \hat{f}_{i+1,j}^{t-1}\|_{H^{-1}(\Omega_{i+1,j}^{\text{PML}})} \\ &\quad + Ck^{\frac{3}{2}}(1+kL) \|u_{i+1,j}^{t-1}\|_{H^{\frac{1}{2}}(\partial\Omega_{i+1,j}^{\text{PML}})}. \end{aligned}$$

Since $u_{i,j}^s = 0$ for $|i-i_0|+|j-j_0|+1 \neq s$, and we have (40) for $|i-i_0|+|j-j_0|+1 = s$ in Lemma 3.2, thus

$$\begin{aligned} \|u_{i+1,j}^{t-1} - \hat{u}_{i+1,j}^{t-1}\|_{H^1(\Omega_{i+1,j}^{\text{PML}})} &\leq Ck^{\frac{3}{2}} \|f_{i+1,j}^{t-1} - \hat{f}_{i+1,j}^{t-1}\|_{H^{-1}(\Omega_{i+1,j}^{\text{PML}})} \\ &\quad + Ck^2(1+kL)^2 e^{-\frac{1}{2}k\gamma_0\bar{\sigma}} \|f_{i_0,j_0}\|_{H^1(\Omega)'}. \end{aligned}$$

Similar estimates also hold for the other terms in the right hand side of (48).

Therefore we have

$$\begin{aligned} \|f_{i,j}^t - \hat{f}_{i,j}^t\|_{H^{-1}(\Omega_{i,j}^{\text{PML}})} &\leq \sum_{(i',j')=(i\pm 1,j),(i,j\pm 1)} Ck^{3/2} \|f_{i',j'}^{t-1} - \hat{f}_{i',j'}^{t-1}\|_{H^1(\Omega_{i',j'}^{\text{PML}})} \\ &\quad + \sum_{(i',j')=(i\pm 1,j+1),(i\pm 1,j-1)} Ck^{3/2} \|f_{i',j'}^{t-2} - \hat{f}_{i',j'}^{t-2}\|_{H^1(\Omega_{i',j'}^{\text{PML}})} \\ &\quad + Ck^2(1+kL)^2 e^{-\frac{1}{2}k\gamma_0\bar{\sigma}} \|f_{i_0,j_0}\|_{H^1(\Omega)'} \\ &\leq Ck^{\frac{3}{2}t-1}(1+kL)^2 e^{-\frac{1}{2}k\gamma_0\bar{\sigma}} \|f_{i_0,j_0}\|_{H^1(\Omega)'}, \end{aligned}$$

thus we have (47) by induction.

Next we will prove (46). For the case $s = 1$, (46) holds by (34), and for the case $s > 1$, it also holds by using standard argument again with (40) and (47). \square

In the above analysis, we deal with the case of only $f_{i_0, j_0} \neq 0$. For the general case, $f = \sum_{i,j} f_{i,j}$, $u(f) = \sum_{i,j} u(f_{i,j})$, thus we have the following result by Lemma 3.3.

Theorem 3.4. *Assume $\sigma_0 d$ is sufficiently large, then it holds*

$$\|u - \hat{u}_{DDM}\|_{H^1(\Omega^{PML})} \leq C k^{\frac{3}{2}N_1 + \frac{3}{2}N_2 + \frac{1}{2}} (1 + kL)^2 e^{-\frac{1}{2}k\gamma_0\bar{\sigma}} \|f\|_{H^1(\Omega)}, \quad (49)$$

where u is the solution to the PML problem \mathcal{P}_Ω with the source f , and \hat{u}_{DDM} is the DDM solution for the corresponding truncated PML problem constructed by Algorithm 3.1.

4 Numerical experiments

We will numerically test our additive overlapping DDM in bounded truncated domains using Algorithm 3.1. First, the convergence of the discrete DDM solutions is tested. From Theorem 3.4, the truncated DDM solution in the continuous case is a good approximation to the solution of the original problem (1) when appropriate PML medium parameters are chosen. With the subdomain problems being discretized by finite difference or finite element method, it is expected that the discretization error usually dominates the total error, and to verify this, we test our method for two and three dimensional problems with constant medium. Second, our DDM will also be tested as an iterative solver (i.e., Algorithm 3.1 could be used as an iterative method in which the total number of iterations/steps is determined by certain convergence/stopping criterion) or as a preconditioner for global discrete systems for large wave number problems. We test Algorithm 3.1 for both some constant medium and layered medium problems to compare their performance.

Five points finite difference scheme in two dimensions and seven points finite difference scheme in three dimensions are respectively taken to discretize the problems (the Laplacian operator) on uniform rectangular meshes, both of them are obviously second order accurate. We have implemented a parallel version of DDM algorithm 3.1 using Message Passing Interface (MPI) and the local subdomain problems are solved with the direct solver “MUMPS” [17]. The supercomputer “Tianhe-2 Cluster” located in Tianjin, China is used for our numerical tests, each node of the cluster has two 2.2GHz Xeon E5-2692 processors with 12 cores, and 64G memory.

4.1 Convergence tests of the discrete DDM solutions

In this subsection, the proposed DDM is tested for the problems with constant medium – with the wave number and the number of subdomains both being fixed, the mesh resolution is increased to test the convergence of the discrete solutions.

4.1.1 2D example

In this example, we solve a two-dimensional Helmholtz problem with a constant wave number $k/2\pi = 25$. The computational domain is $B_L = [-L, L] \times [-L, L]$ with $L = 1/2$, and the interior domain without PML is $B_l = [-l, l] \times [l, -l]$ with $l = 25/56$. Denote q as the mesh density which is the number of nodes per wave length, a serie of meshes are used in the computation where the mesh density is approximately $q \approx 22, 45, 90, 180, 270$, respectively. The domain B_L is partitioned into 5×5 subdomains, and thus the total number of steps used for constructing the DDM solution is $5 + 5 = 10$. The source is chosen as

$$f = \frac{16k^2}{\pi^3} e^{-\left(\frac{4k}{\pi}\right)^2((x-x_0)^2+(y-y_0)^2)},$$

where $(x_0, y_0) = (0.09, 0.268)$, thus it is almost supported by four subdomains $\Omega_{3,4}$, $\Omega_{3,5}$, $\Omega_{4,4}$ and $\Omega_{4,5}$.

Table 1 reports the errors and convergence rates of the discrete DDM solutions for this 2D example, and Figure 6 shows the real part of the simulated DDM solution on the mesh of 6720^2 . It is observed that the errors of the truncated DDM solutions (49) are very small with appropriate medium parameters for PML and the finite difference discretization errors do dominate the total errors. We obtain as expected the optimal second order convergence of the errors measured by the L^2 norm along the refinement of the meshes. Note that we also have super-convergence of the H^1 error. Such behavior was also observed in numerical tests for Poisson problem [39] and proved on rectangular domains [40].

Mesh Size	Local Size without PML	L^2 Error	Conv. Rate	H^1 Error	Conv. Rate
560^2	100^2	3.13×10^{-3}		5.47×10^{-1}	
1120^2	200^2	7.68×10^{-4}	2.0	1.36×10^{-1}	2.0
2240^2	400^2	1.95×10^{-4}	2.0	3.40×10^{-2}	2.0
4480^2	800^2	4.85×10^{-5}	2.0	8.50×10^{-3}	2.0
6720^2	1200^2	2.16×10^{-5}	2.0	3.79×10^{-3}	2.0

Table 1: The errors and convergence rates of the DDM solutions for the 2D constant medium problem.

4.1.2 3D example

Next we solve a three-dimensional Helmholtz problem with a constant wave number $k/2\pi = 10$. The computational domain is still B_L with $L = 1/2$, but the interior domain without PML is B_l with $l = 3/8$. A series of meshes is used in the computation where the mesh density is approximately $q \approx 8, 9.5, 13, 16$, respectively. The domain B_L is partitioned into $3 \times 3 \times 3$ subdomains, and the total number of steps used for constructing the DDM solutions is $3 + 3 + 3 = 9$. The source is chosen as

$$f = \frac{64k^3}{\pi^{9/2}} e^{-\left(\frac{4k}{\pi}\right)^2((x-x_0)^2+(y-y_0)^2+(z-z_0)^2)},$$

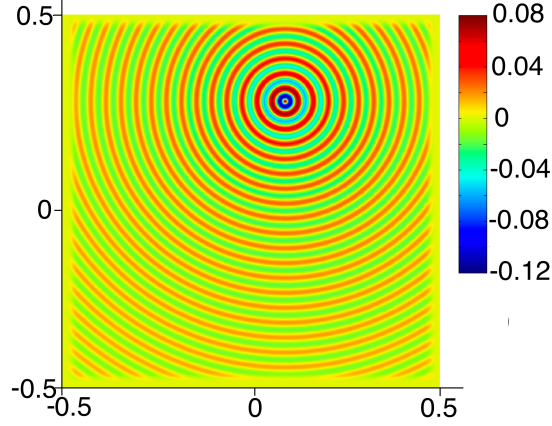


Figure 6: The real part of the simulated DDM solution on the mesh of size 2240^2 for the 2D constant medium problem.

where $(x_0, y_0, z_0) = (0.12, 0.133, 0.125)$, thus it is almost supported by eight subdomains $\Omega_{i,j,m}$ where $i = 2, 3$, $j = 2, 3$, $m = 2, 3$.

Table 2 reports the errors and convergence rates of the discrete DDM solutions for this 3D example, and Figure 7 shows the real part of the simulated solution on the mesh of 160^3 . Again, the finite difference errors dominate the total errors, and we obtain the optimal second order convergence for both L^2 and H^1 errors as expected.

Mesh Size	Local Size without PML	L^2 Errors	Conv. Rate	H^1 Errors	Conv. Rate
80^3	20^3	2.66×10^{-2}		1.82×10^0	
96^3	24^3	1.81×10^{-2}	2.1	1.25×10^0	2.1
128^3	32^3	9.99×10^{-3}	2.1	6.94×10^{-1}	2.0
160^3	40^3	6.39×10^{-3}	2.0	4.45×10^{-1}	2.0

Table 2: The errors and convergence rates of the DDM solutions for the 3D constant medium problem.

4.2 Performance tests with the DDM as an iterative solver or a preconditioner for the global discrete system

The DDM Algorithm 3.1 designed for the constant medium Helmholtz problem also could be used as an iterative solution method for both constant and variable medium problems. More iterations/steps than $N_1 + N_2$ is then usually needed for the iterative solver to reach certain relative error tolerances. We first test the DDM method as an iterative solver for some 2D constant medium and layered medium problems and then as a preconditioner for the global discrete system and compare their performance.

A single shot in the subdomain $\Omega_{1,1}$ is taken as the source with the position

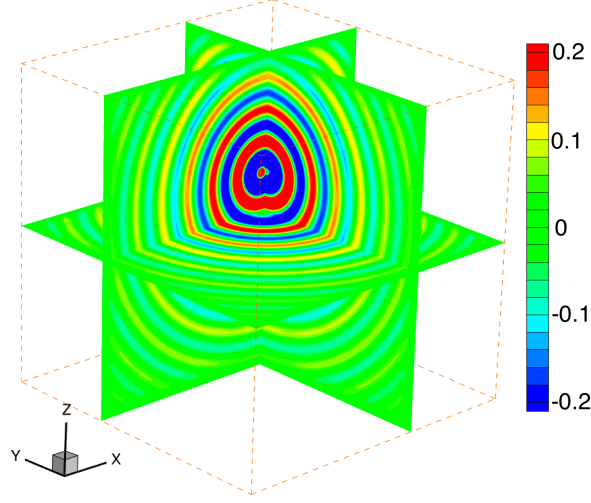


Figure 7: The real part of the simulated DDM solution on the mesh of size 160^3 for the 3D constant medium problem.

being (x^s, y^s) , where

$$x^s = x_0 + \Delta\xi_x/4, \quad y^s = y_0 + \Delta\eta_y/3. \quad (50)$$

Let h_x and h_y denote the mesh sizes in x and y directions, respectively. The shape of the shot is an approximate δ function, defined by

$$f_{i,j} = \frac{1}{h_x h_y} \delta(x^s - i h_x) \delta(y^s - j h_y). \quad (51)$$

The size of the subdomain problems is fixed in all of the following tests, each non-overlapping subregion is of size 300×300 , and the PML layer is 30 points width at each side of the subdomain. The number of subdomains is increased from 2×2 to 32×32 . Denote by $n_{\text{DDM_Iter}}$ the total number of iterations. The number of DDM solve defined by

$$n_{\text{DDM_Solv}} = \frac{n_{\text{DDM_Iter}}}{N_1 + N_2} \quad (52)$$

is used to measure the effectiveness of the iterative solver. It is always highly desired that the number of used iterations $n_{\text{DDM_Iter}}$ for convergence is proportional to $N_1 + N_2$ as the number of subdomains grows, in that case, $n_{\text{DDM_Solv}}$ remains almost the same. The tolerance for relative residuals is set to be 10^{-8} as the stopping criterion for all tests. Note that we also let each subdomain use exactly one core in the following tests.

4.2.1 As an iterative solver

The Algorithm 3.1 is firstly tested as an iterative solver for the global discrete system.

First we test the additive overlapping DDM solver for a constant medium problem on the square domain $[0, 1] \times [-1, 0]$, with different frequencies. The results on the numbers of used iterations and the running times are reported in Table 3. As we can see, the number of DDM solves $n_{\text{DDM_Solv}}$ grows as the number of the subdomains grows from 2×2 to 8×8 , but remains around 1.92 when the number of the subdomains grows further.

Mesh Size	$N_1 \times N_2$	Frequency $\omega/2\pi$	$n_{\text{DDM_Iter}}$	$n_{\text{DDM_Solv}}$	Total Time (sec)	Time/Iter (sec)
600^2	2×2	55	5	1.25	2.0	0.40
1200^2	4×4	105	13	1.63	4.7	0.36
2400^2	8×8	205	29	1.81	11.1	0.38
4800^2	16×16	405	61	1.91	24.4	0.40
9600^2	32×32	805	123	1.92	55.9	0.45
19200^2	64×64	1605	247	1.93	117.2	0.47

Table 3: The performance of the DDM as an iterative solver for the 2D constant medium problem with the subdomain problem size being fixed.

Next we test the DDM solver for a layered medium problem on the square domain $[0, 1] \times [-1, 0]$, as shown in Figure 8 (left) for the velocity profile. For the purpose of illustration, the approximate solution of the problem produced by using the uniform mesh of size 1600^2 is shown in Figure 8 (right). The results

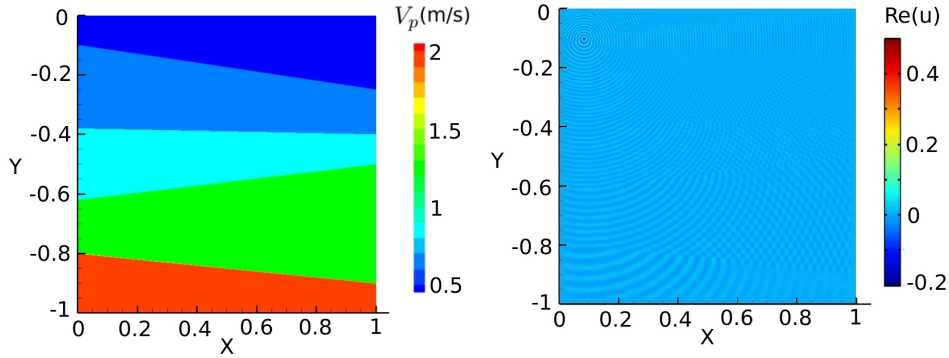


Figure 8: Left: the 2D layered medium velocity profile; right: the real part of discrete solution of the problem on the mesh of size 2400^2 .

on the numbers of used iterations and the running times are reported in Table 4. As we can see, the number of DDM solves almost does not change as the number of the subdomains grows, and it requires about 2.3 times iterations to converge compared with the constant medium problem.

Based on the results on the time cost per DDM iteration with up to $64 \times 64 = 4096$ cores (equivalent to the number of subdomains) reported in Tables 3 and 4, it is easy to see that the proposed additive overlapping DDM is indeed highly scalable and achieve excellent parallel efficiency.

Mesh Size	$N_1 \times N_2$	Frequency $\omega/2\pi$	$n_{\text{DDM_Iter}}$	$n_{\text{DDM_Solv}}$	Total Time (sec)	Time/Iter (sec)
600^2	2×2	27.5	16	4.00	5.7	0.36
1200^2	4×4	52.5	38	4.75	13.2	0.35
2400^2	8×8	102.5	73	4.56	27.8	0.38
4800^2	16×16	202.5	146	4.56	62.4	0.43
9600^2	32×32	402.5	291	4.55	133.1	0.46
19200^2	64×64	802.5	582	4.55	278.8	0.48

Table 4: The performance of the DDM as an iterative solver for the 2D layered medium problem with the subdomain problem size being fixed.

4.2.2 As a preconditioner

Next we use Algorithm 3.1 as a preconditioner to the flexible GMRES (FGMRES) solver for the global discrete system. The number of subdomains is set to 16×16 as an example. Note that when using Algorithm 3.1 as a preconditioner, the number of DDM steps K in each preconditioning solve is to be chosen, we test different K 's for both constant medium and layered medium cases, and the results are reported in Tables 5 and 6. Since the major computational cost during the iterations of solving the linear system is in the back substitute of LU factorization of each subdomain, so the number of back substitutes, denoted as $n_{\text{Local_Solv}}$, is also presented in the tables.

In the constant medium case, both the total running time and $n_{\text{Local_Solv}}$ basically decrease as K increases from 1 to $N_1 + N_2 = 16 + 16 = 32$. It is also easy to see that $n_{\text{Local_Solv}}$ for all cases of K are larger than $n_{\text{DDM_Iter}}$ ($= 61$) used by the DDM iterative solver with 16×16 subdomains (see Table 3), and so does the total time cost (24.4 seconds for the DDM iterative solver). The DDM preconditioner with the largest $K = 32$ achieves almost similar performance as the DDM iterative solver.

In the layered medium case, $n_{\text{Local_Solv}}$ only slightly increase (one exception) from 148 to 160 as K increases. When $K = 1$, although $n_{\text{Local_Solv}}$ is relatively small, the extra cost of GMRES takes more time and the total running time is the largest. When $K = 2$, the best $n_{\text{Local_Solv}}$ ($= 146$) is reached and in fact it equals exactly, $n_{\text{DDM_Iter}}$, the number of iterations needed by the DDM iterative solver with 16×16 subdomains (see Table 4), but the total running time is larger (71.3 vs. 62.4 seconds). For $K \geq 3$, all the time costs are close to 62.4 seconds, which indicates that the performance differences between the DDM preconditioner and the DDM iterative solver are small.

To summarize, it is observed by our experiments that when the additive overlapping DDM is used as a preconditioner, large K should be taken, and its performance is slightly worse than to be used as an iterative solver.

5 Conclusions

In this paper, we propose and analyze an additive overlapping DDM for solving the high-frequency Helmholtz equation. The source transfer technique is used in horizontal, vertical and corner directions, to make the wave propagates away from the source subdomain by subdomain. For the constant medium case, the

K	$n_{\text{GMRES_Iter}}$	$n_{\text{Local_Solv}}$	Total Time (sec)
1	91	91	44.0
2	41	82	39.8
3	27	81	37.8
5	16	80	35.0
10	8	80	33.3
15	5	75	30.7
20	4	80	32.9
32	2	64	26.6

Table 5: The performance of the DDM as a preconditioner to the global FGM-RES solver for the 2D constant medium problem. The number of subdomains is 16×16 .

K	$n_{\text{GMRES_Iter}}$	$n_{\text{Local_Solv}}$	Total Time (sec)
1	148	148	83.7
2	73	146	71.3
3	50	150	68.5
5	30	150	66.1
10	15	150	62.3
15	10	150	60.8
20	8	160	66.9
32	5	160	63.1

Table 6: The performance of the DDM as a preconditioner to the global FGM-RES solver for the 2D layered medium problem. The number of subdomains is 16×16 .

DDM method is shown to exactly solve the PML problem defined in \mathbb{R}^2 , and an error estimation is established for the method used for solving the PML problem in bounded truncated domains. The DDM method could be used as an iterative solver or a preconditioner for the global discrete system in both constant or variable medium problems, and as an iterative solver is more preferable. The method is very suitable for large-scale parallel computing as demonstrated by numerical experiments. Although the method has been extended to three dimensions, error estimation of the method for the truncated PML problem in bounded three-dimensional domains is still open and will be studied in the next step. In addition, we would like to remark that this DDM method could be generalized to irregular domains, with special domain decompositions that require each subdomain to be convex polygons. In such case, the source transfer would be along the outward normal directions of each subdomain boundary. The convergence analysis and performance of such generalized method is also worthy of further investigation.

References

- [1] G. Arfken, *Mathematical Methods for Physicists*, 3rd Ed., Academic Press, 1985.

- [2] J.H. Bramble and J.E. Pasciak, Analysis of a cartesian PML approximation to acoustic scattering problems in R^2 and R^3 , *J. Comput. Math.*, 247 (2013), pp. 209-230.
- [3] J.P. Berenger. A perfectly matched layer for the absorption of electromagnetic waves. *J. Comput. Phys.*, 114(2):185-200, 1994.
- [4] Z. Chen and X. Xiang. A source transfer domain decomposition method for Helmholtz equations in unbounded domain. *SIAM J. Numer. Anal.*, 51(4):2331-2356, 2013.
- [5] Z. Chen and X. Xiang. A source transfer domain decomposition method for Helmholtz equations in unbounded domain Part II: Extensions. *Numer. Math. Theory Methods Appl.*, 6(3):538-555, 2013.
- [6] W.C. Chew and W.H. Weedon. A 3D perfectly matched medium from modified Maxwell's equations with stretched coordinates. *Microw. Opt. Techn. Let.*, 7(13):599-604, 1994.
- [7] Y. Du and H. Wu. An improved pure source transfer domain decomposition method for Helmholtz equations in unbounded domain. *arXiv e-prints*, #1505.06052, Dec. 2016.
- [8] I.S. Duff and J. Reid, The multifrontal solution of indefinite sparse symmetric linear equations, *ACM Trans. Math. Soft.*, 9:302-325, 1983.
- [9] B. Engquist and L. Ying. Sweeping preconditioner for the Helmholtz equation: hierarchical matrix representation. *Comm. Pure Appl. Math.*, 64(5):697-735, 2011.
- [10] B. Engquist and L. Ying. Sweeping preconditioner for the Helmholtz equation: moving perfectly matched layers. *Multiscale Model. Simul.*, 9(2):686-710, 2011.
- [11] M. Gander and F. Nataf. A ILU for Helmholtz problems: a new preconditioner based on the analytic parabolic factorization. *J. Comput. Acoust.*, 9(4):1499-1506, 2001.
- [12] S. Kim and J.E. Pasciak, Analysis of a cartesian PML approximation to acoustic scattering problems in R^2 , *J. Math. Anal. Appl.*, 370 (2010), pp. 168-186.
- [13] W. Leng. A Fast Propagation Method for the Helmholtz equation. *Chinese Journal of Engineering Mathematics*, 32(5):726-742, 2015.
- [14] J. Liu, The multifrontal method for sparse matrix solution: theory and practice, *SIAM Rev.*, 34:82-109, 1992.
- [15] F. Liu and L. Ying. Additive Sweeping Preconditioner for the Helmholtz Equation. *Multiscale Model. Simul.*, 14(2), 799-822, 2016.
- [16] F. Liu and L. Ying. Recursive Sweeping Preconditioner for the 3D Helmholtz Equation. *SIAM J. Sci. Comput.*, 38(2), A814-A832, 2016.

- [17] P.R. Amestoy, I.S. Duff, J. Koster and J.Y. L'Excellent. A fully asynchronous multifrontal solver using distributed dynamic scheduling. *SIAM J. Matrix Anal. Appl.*, 23(1):15-41, 2001.
- [18] C.C. Stolk. A rapidly converging domain decomposition method for the Helmholtz equation. *J. Comput. Phys.*, 241:240-252, 2013.
- [19] A. Vion and C. Geuzaine. Double sweep preconditioner for optimized Schwarz methods applied to the Helmholtz problem. *J. Comput. Phys.*, 266:171-190, 2014.
- [20] M. Gu, J. Xia, S. Chandrasekaran and X.S. Li. Fast algorithms for hierarchically semi-separable matrices, *Numerical Linear Algebra with Applications*, 17(6):953-976, 2010.
- [21] S. Wang, X. Li, F. Rouet, J. Xia, V.H. Maarten. A Parallel Geometric Multifrontal Solver Using Hierarchically Semiseparable Structure. *ACM Trans. Math. Soft.*, 42(3):1-21, 2016.
- [22] L. Zepeda-Núñez and L. Demanet. The method of polarized traces for the 2D Helmholtz equation. *J. Comput. Phys.*, 308:347-388, 2016.
- [23] H.A. Schwarz. Über einen grenzübergang durch alternierendes verfahren. *Vierteljahrsschrift der Naturforschenden Gesellschaft in Zurich*, 15:272-286, 1870.
- [24] P.-L. Lions. On the Schwarz alternating method II. In Tony Chan, Roland Glowinski, Jacques Periaux, and Olof Widlund, editors, *Domain Decomposition Methods, Lecture Notes in Computational Science and Engineering*, pages 47-70. SIAM, 1989.
- [25] B. Després. Décomposition de domaine et problème de Helmholtz. *Comptes rendus de l'Académie des sciences. Série 1, Mathématique*, 311:313-316, 1990.
- [26] Y. Boubendir. An analysis of the BEM-FEM non-overlapping domain decomposition method for a scattering problem. *Journal of Computational and Applied Mathematics*, 204(2):282-291, 2007.
- [27] F. Collino, S. Ghanemi, and P. Joly. Domain decomposition method for harmonic wave propagation: a general presentation. *Computer Methods in Applied Mechanics and Engineering*, 184(24):171-211, 2000.
- [28] A. de La Bourdonnaye, C. Farhat, A. Macedo, F. Magoules, and F.-X. Roux. A non-overlapping domain decomposition method for the exterior Helmholtz problem. *Contemporary Mathematics*, 218:42-66, 1998.
- [29] S. Ghanemi. A domain decomposition method for Helmholtz scattering problems. *Ninth International Conference on Domain Decomposition Methods*, Pages 105-112, 1998.
- [30] F. Magoules, K. Meerbergen, and J.-P. Coyette. Application of a domain decomposition with Lagrange multipliers to acoustic problems arising from the automotive industry. *Computational Acoustics*, 32, 08(03):503-521, 2000.

- [31] L.C. McInnes, R.F. Susan-Resiga, D. E. Keyes, and H. M. Atassi. Additive schwarz methods with nonreflecting boundary conditions for the parallel computation of Helmholtz problems. *Contemporary Mathematics*, 218:325-333, 1998.
- [32] M. Gander. Optimized schwarz methods. *SIAM Journal on Numerical Analysis*, 44(2):699-731, 2006.
- [33] M. Gander, F. Magoulés, and F. Nataf. Optimized Schwarz methods without overlap for the Helmholtz equation. *SIAM Journal on Scientific Computing*, 24(1):38-60, 2002.
- [34] M. Gander and F. Kwok. Optimal interface conditions for an arbitrary decomposition into subdomains. In Yunqing Huang, Ralf Kornhuber, Olof Widlund, and Jinchao Xu, editors, Domain Decomposition Methods in Science and Engineering XIX, *Lecture Notes in Computational Science and Engineering*, 78:101-108. Springer Berlin Heidelberg, 2011.
- [35] M. Gander and H. Zhang. Domain decomposition methods for the Helmholtz equation: A numerical investigation. In Randolph Bank, Michael Holst, Olof Widlund, and Jinchao Xu, editors, Domain Decomposition Methods in Science and Engineering XX, *Lecture Notes in Computational Science and Engineering*, 91:215-222. Springer Berlin Heidelberg, 2013.
- [36] M. Gander and H. Zhang. Domain Decomposition Methods in Science and Engineering XXI, chapter Optimized Schwarz Methods with Overlap for the Helmholtz Equation, Pages 207-215. Springer International Publishing, Cham, 2014.
- [37] M. Gander and Y. Xu. Domain Decomposition Methods in Science and Engineering XXII, chapter Optimized Schwarz Method with Two-Sided Transmission Conditions in an Unsymmetric Domain Decomposition, Pages 631-639. Springer International Publishing, Cham, 2016.
- [38] Y. Boubendir, X. Antoine, and C. Geuzaine. A quasi-optimal non-overlapping domain decomposition algorithm for the Helmholtz equation. *Journal of Computational Physics*, 231(2):262-280, 2012.
- [39] Y.T. Ng, H. Chen, C. Min, F. Gibou. Guidelines for Poisson solvers on irregular domains with Dirichlet boundary conditions using the ghost fluid method. *J. Sci. Comput.* 41:300-320, 2009.
- [40] J.C. Strikwerda. Finite Difference Schemes and Partial Differential Equations. SIAM, Philadelphia, 2004.